Hyperfine Interact (2009) 193:61–67
DOI 10.1007/s10751-009-0062-1

Line shape of the μH($3p - 1s$) transition

D. S. Covita · D. F. Anagnostopoulos · H. Gorke · D. Gotta · A. Gruber · A. Hirtl · T. Ishiwatari · P. Indelicato · E.-O. Le Bigot · M. Nekipelov · J. M. F. dos Santos · Ph. Schmid · L. M. Simons · M. Trassinelli · J. F. C. A. Veloso · J. Zmeskal

Published online: 2 September 2009

Abstract The line shape of the $(3p - 1s)$ X-ray transition in muonic hydrogen was measured for the first time with a high-resolution crystal spectrometer. The assumption of a statistical population of the hyperfine levels was directly confirmed by experiment, and a measured value for the hyperfine splitting is reported. An X-ray line broadening due to Doppler effect could be clearly identified and attributed to different Coulomb de-excitation transitions which precede the measured radiative transition. The results allow a decisive test of advanced cascade model calculations and establish an alternative and "model free" method to extract the strong-interaction parameters from pionic hydrogen data.

Keywords Exotic atoms and molecules · Exotic atoms spectroscopy

D. S. Covita (✉) · J. M. F. dos Santos · L. M. Simons
Dept. of Physics, Coimbra University, 3000 Coimbra, Portugal
e-mail: dscasegas@gian.fis.uc.pt

D. S. Covita · L. M. Simons
Paul Scherrer Institut (PSI), 5232, Villigen, Switzerland

D. F. Anagnostopoulos
Dept. of Materials Sci. and Eng., University of Ioannina, Ioannina, 45110, Greece

H. Gorke · D. Gotta · M. Nekipelov
Forschungszentrum Jülich GmbH and JHCP, 52425 Jülich, Germany

A. Gruber · A. Hirtl · T. Ishiwatari · Ph. Schmid · J. Zmeskal
SMI, Austrian Academy of Sciences, 1090 Vienna, Austria

P. Indelicato · E.-O. Le Bigot · M. Trassinelli
LKB, UPMC-Paris 6, ENS, CNRS; Case 74, 4 place Jussieu, 75005 Paris, France

J. F. C. A. Veloso
Dept. of Physics, Aveiro University, 3810 Aveiro, Portugal

PACS 36.10.-k

1 Introduction

An exotic atom is formed by capture of a negatively charged particle in the Coulomb field of a nucleus into high-lying atomic states. In the case of hydrogen the subsequent de-excitation cascade is determined by the competition of collisional and radiative processes. One of these collisional processes is the so-called Coulomb de-excitation [1–4], where the released energy is shared between the exotic atom and a hydrogen atom. Therefore, exotic hydrogen systems can be accelerated via these Coulomb transitions leading to a Doppler broadening of X-ray transitions. The spectral lines develop tails up to the maximum Doppler shift given by preceding Coulomb transitions (Table 1). Evidence of a Doppler broadening of X-ray transitions was observed in experiments measuring the strong-interaction width of the pionic hydrogen ground state [5, 6]. Unfolding this contribution is obviously crucial in order to extract the pure hadronic contribution from the πH and πD X-ray line shapes [7, 8].

In order to describe the development of the kinetic energy of exotic hydrogen, which is beyond the Standard Cascade Model (SCM) [9–11], the so-called extended standard cascade model (ESCM) has been developed [12–14]. An example of the kinetic energy distribution calculated for μH in the $3p$ state by ESCM is shown in Fig. 1. The monoenergetic lines corresponding to specific Coulomb transitions $n \rightarrow n'$ are smeared out because of numerous elastic collisions.

Muonic hydrogen is an ideal candidate for direct observation of the Coulomb de-excitation. Any additional broadening of a measured X-ray besides the intrinsic experimental resolution is caused by Doppler effect due to Coulomb de-excitation. Hence, the validity of ESCM is tested by reproducing the line shape of muonic hydrogen X-ray transitions in a fitting routine with the predictions of ESCM as input. Theoretical values for the ground-state hyperfine splitting ΔE_{HFS}, and more important, for the relative intensity of the transitions feeding the triplet and singlet components should be obtained. ΔE_{HFS} is calculated to be 182.725 ± 0.062 meV [15], and a relative statistical population of 3:1 is expected.

2 Experimental conditions

The measurement was performed at the πE5 channel of the Paul Scherrer Institut (PSI) using a 112 MeV/c pion beam injected into the cyclotron trap II [16]. The pions where decelerated inside the cyclotron trap II and forced to spiral into a cryogenic target placed at the center. The target cell was filled with hydrogen gas at a density equivalent of 12.5 bar at room temperature. Muonic atoms are formed by slow muons originating from the decay of almost stopped pions close or inside the target cell.

X-rays from the μH$(3p - 1s)$ transition were measured with a Johann-type Bragg spectrometer equipped with a spherically bent Si (111) crystal and a large-area X-ray detector consisting of a 3×2 array of charge-coupled devices (CCDs) [17]. The crystal with a radius of curvature of 2982.2 ± 0.3 mm and a free diameter of 90 mm was used [18]. The background rejection capability of the CCDs together with

Table 1 Maximum Doppler shift of various μH spectral lines due to Coulomb de-excitation for $\Delta n = 1$ transitions

Spectral line	Max. Doppler shift [eV]	Coulomb transition	Kinetic energy gain [eV]
Kα	$\pm$1.1	$3 \rightarrow 2$	166.3
Kβ	$\pm$0.75	$4 \rightarrow 3$	58.2
Kγ	$\pm$0.54	$5 \rightarrow 4$	29.6
Kδ	$\pm$0.41	$6 \rightarrow 5$	14.6
Kϵ	$\pm$0.32	$7 \rightarrow 6$	8.8

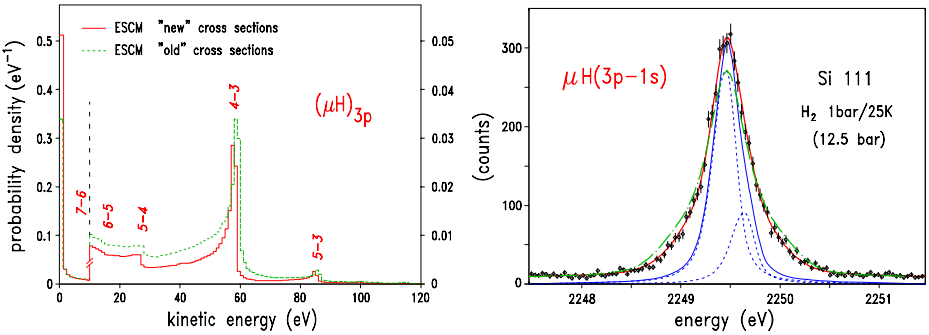

Fig. 1 *Left*: Kinetic energy distribution of μH atoms in the $3p$ state for a hydrogen density of 12.5 bar as predicted from ECSM [12–14] using a) cross sections calculated by [12–14] (*dashed curve*) and b) recalculated cross sections [25] stimulated by the present experiment (*solid curve*). *Numbers* indicate the corresponding Coulomb transitions $n \rightarrow n'$. Note the change of the vertical scale at 10 eV. *Right*: line shape of the μH($3p-1s$) transition as measured with a Si (111) crystal in first order. The spectrometer response (*thin solid line*) represents the expected line shape formed by the two hyperfine components (*dashed lines*). Using a kinetic energy distribution calculated within ESCM approach and including Coulomb de-excitation derived from long standing cross sections [12–14] yields only a poor description (*dashed-dotted*) of the line shape. The "best fit" in the "model free" approach is shown by the thick solid line following the data. An even better fit—being indistinguishable by eye from the "model free" approach—was obtained when using the recently recalculated cross sections [25]

a massive concrete shielding suppresses efficiently background events from beam induced reactions. In total, almost 10000 events were collected for the μH($3p-1s$) line (Fig. 1).

3 Analysis and results

The spin-averaged μH($3p-1s$) transition energy is calculated to be 2249.461 ± 0.001 eV with a radiative line width of 0.3 μeV (Indelicato, unpublished manuscript). The $3p$-level splittings amount to a few meV only [19]. Hence, two components with identical response functions are sufficient to describe the ($3p-1s$) line.

The response function of the crystal spectrometer was measured by using X-rays from Helium-like ions, which were produced in a dedicated electron-cyclotron resonance ion trap (ECRIT) set up at PSI [20, 21]. Helium-like phosphorus, corresponding to the energy of the μH($3p-1s$) X-ray transition, could not be measured because the handling of the phosphorus gases turned out to be too dangerous. Thus,

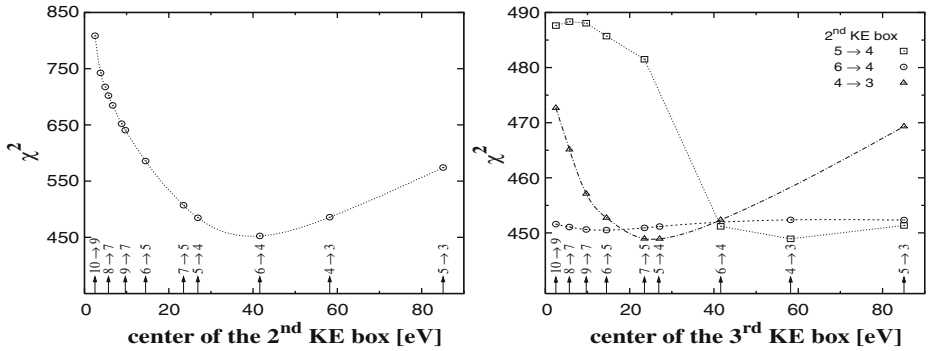

Fig. 2 Search for the position of the 2nd (*left*) and 3rd (*right*) kinetic energy boxes (see text). The kinetic energy gains from the respective Coulomb de-excitation are indicated

the response function at this energy was extrapolated from the results for M1 X-rays of Helium-like sulfur, chlorine and argon yielding a resolution of 272 ± 3 meV (FWHM) [22], which is significantly narrower than the observed total line width (Fig. 1).

When using the kinetic energy distribution given by ESCM of [12–14], the observed line shape cannot be reproduced (Fig. 1). The result reveals that the relative weight of the exotic systems with low-energy ($T_{kin} \leq 2$ eV) should be much larger, *i.e.*, the fraction of X-rays with small Doppler shifts is underestimated.

As an alternative, a "model free" method was applied. It has already been used in the analysis of the time-of-flight (TOF) spectra [23], where rectangular boxes approximate the kinetic energy distribution at the instant of the X-ray. Number and position of the boxes are chosen according to the Coulomb transitions possible in the preceding cascade. Boxes corresponding to Coulomb transitions with $\Delta n = 1, 2$ were admitted. In a first step, the number of boxes and their limits were studied. Both hyperfine components, their relative population, (flat) background and the relative weight of the boxes were free parameters in the fit. The sum of the relative weights of the boxes is always normalized to one.

The presence of a low-energy box, which covers kinetic energies from 0 up to a few eV and with a relative weight close to 60% turned out to be mandatory. It corresponds to μH atoms which arrive at $n = 3$ with their kinetic energy gained only at the upper levels of the cascade ($n \geq 10$) and/or to systems of larger kinetic energy degraded by elastic collisions. An upper limit of 1.8 eV was found to be the best choice for the low-energy component.

The position of higher-energy components was studied by using very narrow boxes with only 1 eV width, centered at the corresponding kinetic energy gain from $\Delta n = 1, 2$ Coulomb de-excitations. At first, with only two boxes, the candidate for a second box was identified. Subsequently, a series with three kinetic energy boxes was performed with the best "second box" candidate found previously.

A χ^2 analysis shows that the fit improves significantly when using, besides the low-energy component, a second box placed between 20 and 60 eV (Fig. 2). It covers the range of the kinetic energy gain owing to the $n = 5 \rightarrow 4$ ($T_{kin} = 26.9$ eV), $n = 6 \rightarrow 4$ ($T_{kin} = 41.6$ eV), and $n = 4 \rightarrow 3$ ($T_{kin} = 58.2$ eV) Coulomb transitions. With

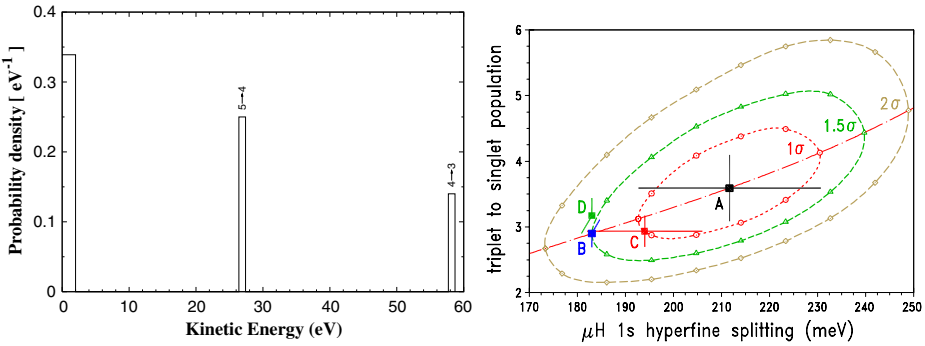

Fig. 3 *Left*: the three kinetic energy boxes found in the "model free" approach to describing correctly the μH($3p-1s$) X-ray line shape. *Right*: χ^2 contour for the correlation of hyperfine splitting and relative population in the "model free" approach. The *dashed-dotted line* displays the location of the minimum χ^2 for the corresponding hyperfine splitting. (*A–D*: see text)

two boxes the minimum $\chi^2/dof = 452.410/475$ is found when placing the 2nd box at $T_{kin} = 41.6\,\text{eV}$ ($n = 6 \rightarrow 4$).

By introducing a 3rd box the fit quality is further improved. Using from the two-component fit 41.6 eV to center the 2nd one, the fit is not sensitive to the position of any 3rd box. In the other two cases, 26.9 and 58.2 eV, however, it is. The minimum $\chi^2/dof = 448.933/474$ is found at the kinetic energy corresponding to the $n=5\rightarrow 4$ and $n=4\rightarrow 3$ transitions for the 2nd and 3rd box (Fig. 2). Therefore, 26.9 eV and 58.2 eV were chosen to place a 2nd and 3rd kinetic energy boxes. When including a fourth box, a similar χ^2 analysis yields no further improvement (less than 0.2 χ^2 units).

Investigating the limits of the high-energy boxes by extending their boundaries up to $\pm 30\%$ of the central values, the results are affected by less than 1.4 standard deviations. Therefore, the kinetic energy distribution was kept condensed to three narrow intervals (Fig. 3): [0–1.8], [26.4–27.4], and [57.7–58.7] eV: one low-energy component and two from the Coulomb de-excitation steps $n = 5 \rightarrow 4$ and $n = 4 \rightarrow 3$ with the relative weights of $(61 \pm 2)\%$, $(25 \pm 3)\%$, and $(14 \pm 4)\%$. Uncertainties represent statistical errors only. The "best fit" in the "model free" approach is also shown in Fig. 1.

By using the three kinetic energy boxes found previously, a systematic study on the correlation between the hyperfine splitting and the relative population was performed. During this procedure the position of the triplet component 1^3S_1, the hyperfine splitting and the relative population were changed in small steps. Hence, only the weights of the boxes, the total intensity and the background were kept as free parameters during the χ^2 optimization. Hyperfine splitting and population ratio were changed in steps of 9.3 meV and 0.5 around their theoretical/statistical values. For each combination, a χ^2 distribution curve, function of the 1^3S_1 position, was obtained. The 1^3S_1 position was changed in steps of 1.9 meV. From the minima of the χ^2 curves, a correlation contour between hyperfine splitting and relative population is constructed. The 1, 1.5, and 2 σ contours are shown in Fig. 3 as well as the location of the χ^2 minima.

The best $\chi^2/dof = 448.903/477$ is obtained for $\Delta E_{HFS} = 211 \pm 19$ meV and a triplet to singlet population of $(3.59 \pm 0.51) : 1$ (Fig. 3–A). Errors correspond to 1σ. When fixing ΔE_{HFS} to the theoretical value, the best fit is found for a triplet to singlet population of $(2.90 \pm 0.21) : 1$ (Fig. 3–B) which is very close to the statistical value and results in a χ^2 only $1.5\,\sigma$ away from the best fit value.

Following the presented results cross-sections involved in the de-excitation cascade of the exotic hydrogen were recalculated. The Coulomb de-excitation, elastic scattering and Stark transitions have been now treated in a unified manner under a quantum-mechanical close-coupling approach [2–4, 24].

By using these cross-sections in the ESCM model [25], the relative weight of the low-energy component ($T_{kin} \leq 2$ eV) increases from about 36% to 55%, which agrees with the constraint found within the "model free" method. Using the new kinetic energy distribution yields a much better description of the data (Fig. 1). Leaving hyperfine splitting and triplet to singlet intensity ratio as free parameters, values of $\Delta E_{HFS} = 194 \pm 12$ meV and $(2.94 \pm 0.24) : 1$ for the triplet to singlet intensity ratio were acquired (Fig. 3–C). When fixing the splitting to the theoretical value the relative triplet to singlet population becomes $(3.17 \pm 0.27) : 1$ (Fig. 3–D).

4 Summary

The line shape of the μH$(3p - 1s)$ transition was measured with a high resolution Bragg spectrometer. The influence of Coulomb de-excitation was directly seen from a line broadening compared to the spectrometer resolution. By using a "model free" approach based on kinetic energy boxes various Doppler contributions are identified, which are attributed to preceding Coulomb transitions. A large fraction of the μH systems are found to have kinetic energies below 2 eV. The measurement yields the μH ground-state hyperfine splitting as calculated from QED within 1.5σ and confirms the statistical population of the triplet and singlet $1s$ states. The "model free" method was validated to be applied also in the πH analysis. The measurement triggered a new calculation of cross sections resulting in a significantly improved description of the μH$(3p - 1s)$ line shape.

Acknowledgements The authors would like to thank V. P. Popov and V. N. Pomerantsev for the possibility to use their recent theoretical development. The continuous theoretical support of V. E. Markushin and T. S. Jensen is gratefully acknowledged. We would like to thank B. Leoni, N. Dolfus, L. Stohwasser, and K.-P. Wieder for the technical assistance. The Bragg crystal was manufactured by Carl Zeiss AG, Oberkochen, Germany. Partial funding and travel support was granted by FCT (Lisbon) and FEDER (PhD grant SFRH/BD/18979/2004 and project PTDC/FIS/82006/2006) and the Germaine de Staël exchange program. This work is part of the PhD thesis of one of us (D. S. C., Univ. of Coimbra, 2008).

References

1. Bracci, L., Fiorentini, G.: Nuovo Cim., A **43**, 9 (1978)
2. Korenman, G.Ya., Pomerantsev, V.N., Popov, V.P.: JETP Lett. **81**, 543 (2005)
3. Pomerantsev, V.N., Popov, V.P.: JETP Lett. **83**, 331 (2006)
4. Pomerantsev, V.N., Popov, V.P.: Phys. Rev., A **73**, 040501(R) (2006)
5. Schröder, H.-Ch., et al.: Eur. Phys. J., C **21**, 473 (2001)
6. Gotta, D., et al.: Lect. Notes Phys. **745**, 165 (2008)

7. Covita, D., et al.: These proceedings
8. Strauch, Th., et al.: These proceedings
9. Leon, M., Bethe, H.A.: Phys. Rev. **127**, 636 (1962)
10. Borie, E., Leon, M.: Phys. Rev., A **21**, 1460 (1980)
11. Reifenröther, G., Klempt, E.: Nucl. Phys., A **503**, 885 (1989)
12. Jensen, T.S., Markushin, V.E.: Eur. Phys. J., D **19**, 165 (2002)
13. Jensen, T.S., Markushin, V.E.: Eur. Phys. J., D **21**, 261 (2002)
14. Jensen, T.S., Markushin, V.E.: Eur. Phys. J., D **21**, 271 (2002)
15. Martynenko, A.P., Faustov, R.N.: JETP **98**, 39 (2004)
16. PSI proposal R-98-01: www.fz-juelich.de/ikp/exotic-atoms
17. Nelms, N., et al.: Nucl. Instrum. Methods A **484**, 419 (2002)
18. Gotta, D.: Prog. Part. Nucl. Phys. **52**, 133 (2004)
19. Pachucki, K.: Phys. Rev., A **53**, 2092 (1996)
20. Anagnostopulos, D.F., et al.: Nucl. Instrum. Methods A **545**, 217 (2005)
21. Trassinelli, M., et al.: J. Phys. Conf. Ser. **58**, 129 (2007)
22. Covita, D.S.: Thesis, Univ. of Coimbra (2008)
23. Badertscher, A., et al.: Europhys. Lett. **54**, 313 (2001), and references therein
24. Popov, V.P., Pomerantsev, V.N.: arXiv:0712.3111v1 [nucl-th] (2007)
25. Jensen, T.S., Pomerantsev, V.N., Popov, V.P.: arXiv:0712.3010v1 [nucl-th] (2007)